An Integrated Mathematical Model of Fluid Dynamics, Heat Transfer and Reaction Kinetics for Fluidized Bed Gasification of Sorghum DDG

Lijun Wang, Curtis L. Weller and Milford A. Hanna

Industrial Agricultural Products Center, Department of Biological Systems Engineering, University of Nebraska-Lincoln, Lincoln, NE 68583-0726, USA

Abstract

A transient and three-dimensional mathematical model was developed to investigate the fluidized bed gasification of biomass (sorghum DDG). The materials in the gasifier were composed of fluidizing gas, DDG particles and sand. The fluid flow inside the gasifier was described using the Navier-Stokes equations. Turbulence of the flow was taken into account using a k - ε model. Conversion rate of biomass was determined using a kinetics scheme. A user-friendly computer program was developed to implement the model. The model was solved using a finite element method.

Keywords: fluidized bed gasification, biomass, bioenergy, computational fluid dynamics, mathematical modeling, and finite element

1. Introduction

Dry-grind ethanol production continues to expand in the United States. More than 50 million bushels of grain sorghum are used annually to produce ethanol and the number is expected to increase in the future. Approximately 18 pounds of dry residual in form of distillers dried grain (DDG) remains from each bushel of grain sorghum used to produce ethanol. The powdery sorghum DDG has a lipid content as high as 9.5% (dry basis) including valuable components such as phytosterols, tocols and diacylglycerols (Wang et al., 2005). The economic value of DDG would likely increase if the lipid materials were extracted from the DDG and the solid DDG residue after extraction was further converted to fuels and chemicals.

Thermochemical conversion technologies such as pyrolysis and gasification have been used to produce fuels and chemicals from agricultural and forest residues (Lanzetta and Blasi, 1998; Rapagna et al., 2000; Lv et al., 2003). Compared with a traditional fixed bed gasifier, a fluidized bed gasifier has the advantages of more flexibility in feedstock, lower capital and operating cost, and lower oxygen consumption. Although numerous experimental analyses on fluidized bed gasification of biomass are available (Rapagna et al., 2000; Lv et al., 2003), there is a lack of detailed physical understanding and predictive tools for the design and optimization of fluidized bed gasifiers for biomass. Research on reaction kinetics, heat transfer and fluid dynamics in a fluidized bed gasifier is important to optimize gasifier design and operating conditions for further improving conversion efficiency of the system and quality of produced gas.

Fluidized bed gasification can be characterized by its time-dependent, turbulent, multi-phase, multi-dimensional, and reactive fluid flow. The flow experiences multiple modes of heat transfer and complex chemical reaction. Transport phenomena are coupled with chemical reactions. Due to high temperature, velocity and species gradients inside the gasifier, there are large material property variations during gasification. Fluidized bed gasification modeling and

simulation is a new field compared to the modeling of combustion processes. Lathououwers and Bellan (2001) developed a two-dimensional mathematical model for the description of fluidized bed pyrolysis of biomass. However, a two-dimensional model cannot adequately describe the complex behaviors of multiphase fluids in a gasifier. Multi-dimensional modeling can provide important insight into fluid behavior that is impossible to describe with simpler geometrical models.

The objective of this research was to develop a transient and three-dimensional mathematical model to investigate the fluid flow, heat transfer and gasification kinetics during fluidized bed gasification of grain sorghum DDG. The integrated model may provide a cheaper and a faster tool for the design, operation, control and scale-up of a fluidized bed gasifier of biomass.

2. Mathematical Model

The materials in the gasifier were composed of sorghum DDG particles, sand and fluidizing gas. Cellulose, hemicellulose and lignin were assumed to be the three main components of sorghum DDG. Products of gasification include syngas mixture, tar and char. The physical processes occurring during fluidized bed gasification of biomass are shown in Figure 1. To predict the behavior of biomass in a gasifier, the process chemistry had to be coupled with transport phenomena. The model included three sub-models to describe (1) fluid dynamics of three phases, (2) heat transfer among three phases, and (3) temperature-dependent reaction kinetics of the conversion from the three main components of sorghum DDG to products. Numerical solutions to the model were found using a finite element scheme with a set of input parameters.

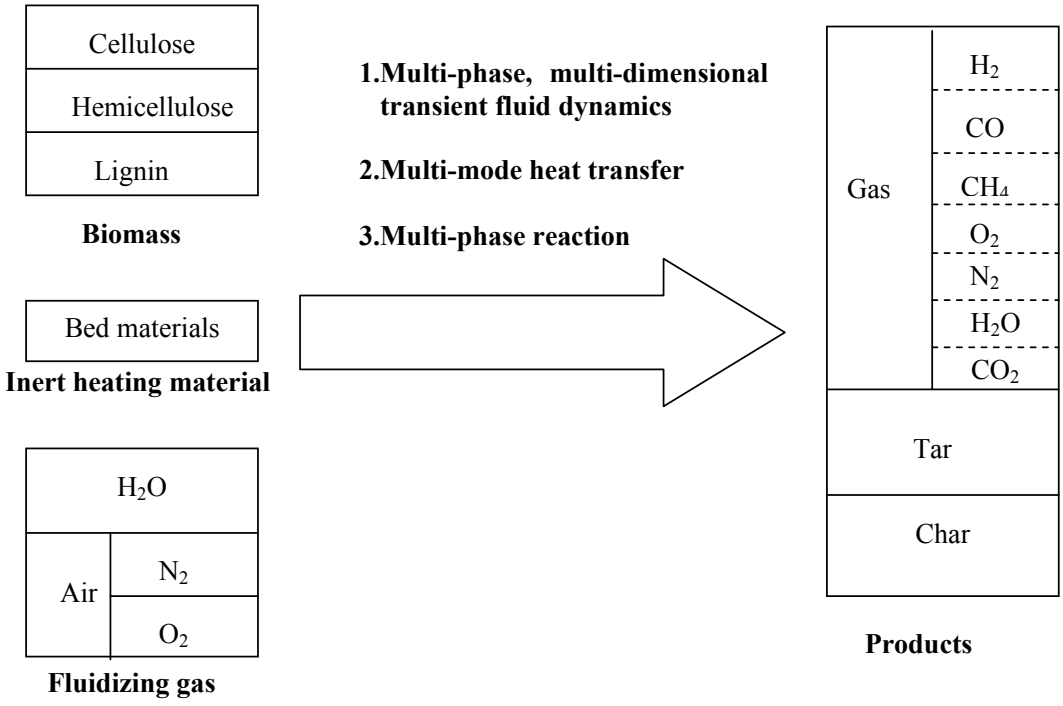

Figure 1. Physical mechanism of fluidized bed gasification of biomass.

2.1 Fluid dynamics

A set of Navier-Stokes equations including one continuity equation and three momentum equations were used to describe the fluid flow of each phase. Therefore, there are 12 partial differential equations for the description of fluid flow of three phases. The interactions among three phases were considered as source terms in the Navier-Stokes equations.

The general continuity equation used to describe the mass conservation of carrier gas, biomass and inert heating particles was

$$\frac{\partial}{\partial t}(\sigma\rho)_i + \nabla \cdot (\sigma\rho U)_i = S_{M,i} \tag{1}$$

where *i* denotes carrier gas (g), biomass (b) and inert heating particles (h), U is velocity vector (u, v, w), σ is volumetric fraction, ρ is density, and S_M is the source term.

The densities of biomass and inert heating particles were assumed to be constant during gasification. The gas was compressible. The density of gas phase was a function of pressure and temperature, which was calculated using the ideal gas law:

$$\rho_g = \frac{PM_g}{RT} \tag{2}$$

During gasification, the mass reduction rate of biomass particles was equal to the mass increasing rate of gas:

$$-S_{M,b} = S_{M,g} \tag{3}$$

$$S_{M,b} = (\sigma\rho)_b \sum_j R_{bj} \tag{4}$$

In the above equation, R_{bj} (kg reacted component /s·kg biomass) was the reaction rate of the j^{th} component in the biomass. The reaction rates were determined in the section of reaction kinetics below. For the inert heating particle, there was no mass reduction or production:

$$S_{M,h} = 0 \tag{5}$$

The momentum conservation of each phase in three directions was expressed as (Versteeg and Malalasekera, 1995):

$$\frac{\partial}{\partial t}(\sigma\rho u)_i + \nabla \cdot (\sigma\rho u U)_i = -\left(\sigma \frac{\partial P}{\partial x}\right)_i + \nabla \cdot (\sigma\mu_e \nabla u)_i + S_{F,i,x} \text{ (x-momentum)} \tag{6}$$

$$\frac{\partial}{\partial t}(\sigma\rho v)_i + \nabla \cdot (\sigma\rho v U)_i = -\left(\sigma \frac{\partial P}{\partial y}\right)_i + \nabla \cdot (\sigma\mu_e \nabla v)_i + S_{F,i,y} \text{ (y-momentum)} \tag{7}$$

$$\frac{\partial}{\partial t}(\sigma\rho w)_i + \nabla\cdot(\sigma\rho w U)_i = -\left(\sigma\frac{\partial P}{\partial z}\right)_i + \nabla\cdot(\sigma\mu_e\nabla w)_i + S_{F,i,z} \quad \text{(z-momentum)} \tag{8}$$

where i denotes carrier gas, biomass and inert heating particles, U is the velocity vector of (u, v, w), P is pressure, and S_F is the source term.

The carrier gas, biomass and inert heating particles experienced the gravitational body force and a drag force due to the momentum exchange between the gas phase and solid phase. The gravitational and drag forces were included in the source terms of momentum equations for each phase, which were listed in Table 1.

Table 1. Source terms of each momentum equation for each phase

Phase	Momentum Equation	Source term
Gas	u	$S_{F,g,x} = (-1)\times[\frac{3}{4}\frac{C_{d,b,x}}{d_{p,b}}\sigma_b\rho_g\lvert u_g-u_b\rvert(u_g-u_b) + \frac{3}{4}\frac{C_{d,h,x}}{d_{p,h}}\sigma_h\rho_g\lvert u_g-u_h\rvert(u_g-u_h)]$
	v	$S_{F,g,y} = (-1)\times[\frac{3}{4}\frac{C_{d,b,y}}{d_{p,b}}\sigma_b\rho_g\lvert v_g-v_b\rvert(v_g-v_b) + \frac{3}{4}\frac{C_{d,h,y}}{d_{p,h}}\sigma_h\rho_g\lvert v_g-v_h\rvert(v_g-v_h)]$
	w	$S_{F,g,z} = (-1)\times[\sigma_g\rho_g g + \frac{3}{4}\frac{C_{d,b,z}}{d_{p,b}}\sigma_b\rho_g\lvert v_g-v_b\rvert(v_g-v_b) + \frac{3}{4}\frac{C_{d,h,z}}{d_{p,h}}\sigma_h\rho_g\lvert w_g-w_h\rvert(w_g-w_h)]$
Biomass	u	$S_{F,b,x} = \frac{3}{4}\frac{C_{d,b,x}}{d_{p,b}}\sigma_b\rho_g\lvert u_g-u_b\rvert(u_g-u_b)$
	v	$S_{F,b,y} = \frac{3}{4}\frac{C_{d,b,y}}{d_{p,b}}\sigma_b\rho_g\lvert v_g-v_b\rvert(v_g-v_b)$
	w	$S_{F,b,z} = \sigma_b\rho_b g + \frac{3}{4}\frac{C_{d,b,z}}{d_{p,b}}\sigma_b\rho_g\lvert w_g-w_b\rvert(w_g-w_b)$
Inert heating material	u	$S_{F,h,x} = \frac{3}{4}\frac{C_{d,h,x}}{d_{p,h}}\sigma_h\rho_g\lvert u_g-u_h\rvert(u_g-u_h)$
	v	$S_{F,h,y} = \frac{3}{4}\frac{C_{d,h,y}}{d_{p,h}}\sigma_h\rho_g\lvert v_g-v_h\rvert(v_g-v_h)$
	w	$S_{F,h,z} = \sigma_h\rho_h g + \frac{3}{4}\frac{C_{d,h,z}}{d_{p,h}}\sigma_b\rho_g\lvert w_g-w_h\rvert(w_g-w_h)$

In Table 1, $d_{p,b}$ and $d_{p,h}$ are the diameter of biomass and inert heating material (sand) particles. $C_{d,b}$ and $C_{d,h}$ are the drag coefficient of fluidizing gas imposed on biomass and bed materials particles. The single particle drag coefficient was calculated by (Ishii and Zuber, 1979):

$$C_{d,i} = \frac{24}{\mathrm{Re}_i}\left(1 + 0.1\,\mathrm{Re}_i^{0.75}\right) \tag{9}$$

The Reynolds number in the above equation was given by:

$$\mathrm{Re}_i = \frac{\sigma_g \rho_g d_{p,i} \left| U_g - U_i \right|}{\mu_{e,g}} \tag{10}$$

where i denotes biomass and inert heating material particles, and U is the velocity of u, v or w.

There were 13 unknowns presented in the continuity and momentum equations, which included three volumetric fractions of each phase (σ_g, σ_b, and σ_h), pressure (P), and nine velocities (u, v and w for three phases). An additional closure equation (11) was used to accompany the 12 partial differential continuity and momentum equations to find the 13 unknowns:

$$\sigma_g + \sigma_b + \sigma_h = 1 \tag{11}$$

Turbulence had an effect on the gas viscosity. An efficient gas viscosity was used, which included average and fluctuating terms:

$$\mu_e = \mu + \mu_T \tag{12}$$

The k-ε turbulence model was used to calculate the local turbulent viscosity:

$$\mu_T = C_\mu \rho_g \frac{\kappa^2}{\varepsilon} \tag{13}$$

The conservation equations for the gas turbulent kinetic energy, κ, and turbulent dissipation, ε, were expressed as:

$$\frac{\partial}{\partial t}\left(\sigma\rho\kappa\right)_g + \nabla\cdot\left(\sigma\rho U\kappa\right)_g = \nabla\cdot\left(\sigma\left(\mu + \frac{\mu_t}{\sigma_k}\right)\nabla\kappa\right)_g + \sigma_g\left(G - \rho\varepsilon\right)_g \tag{14}$$

$$\frac{\partial}{\partial t}\left(\sigma\rho\varepsilon\right)_g + \nabla\cdot\left(\sigma\rho U\varepsilon\right)_g = \nabla\cdot\left(\left(\mu + \frac{\mu_t}{\sigma_\varepsilon}\right)\nabla\varepsilon\right)_g + \sigma_g\left(C_{1\varepsilon}\frac{\varepsilon}{k}G - C_{2\varepsilon}\rho\frac{\varepsilon^2}{\kappa}\right)_g \tag{15}$$

where G is a turbulence production term.

The constants in Eqns (13) – (15) are

$C_\mu = 0.09$, $C_{1\varepsilon} = 1.44$, $C_{2\varepsilon} = 1.92$, $\sigma_k = 1.0$ and $\sigma_\varepsilon = 1.3$.

2.2 Heat transfer

The governing equation of energy conservation for the gas phase was given by:

$$\frac{\partial}{\partial t}\left(\sigma\rho c_p T\right)_g + \nabla\cdot\left(\sigma\rho c_p TU\right)_g = \nabla\cdot\left(\sigma k\nabla T\right)_g + S_{E,C} + S_{E,P} \tag{16}$$

where $S_{E,C}$ and $S_{E,P}$ are the body heat sources due to heat exchanges between gas and particles by convection and mass exchange.

The biomass particles experienced heat exchange between the particles and the gas phase by convection ($S_{E,C,b}$) and product release ($S_{E,P}$), thermal radiation ($S_{E,Rd,b}$) and heat of reaction ($S_{E,Re}$). The governing equation of energy conservation for the biomass phase was given by:

$$\frac{\partial}{\partial t}\left(\sigma\rho c_p T\right)_b + \nabla\cdot\left(\sigma\rho c_p TU\right)_b = S_{E,C,b} + S_{E,P} + S_{E,Rd,b} + S_{E,\mathrm{Re}} \tag{17}$$

The inert heating material particles experienced heat exchange between the particles and the gas phase by convection ($S_{E,C,h}$), and thermal radiation ($S_{E,Rd,h}$). The governing equation of energy conservation for the inert heating particles was given by:

$$\frac{\partial}{\partial t}\left(\sigma\rho c_p T\right)_h + \nabla\cdot\left(\sigma\rho c_p TU\right)_h = S_{E,C,h} + S_{E,Rd,h} \tag{18}$$

Each mode of heat transfer in Eqns (16) – (18) was determined as follows:

$$S_{E,C} = S_{E,C,b} + S_{E,C,h} \tag{19}$$

$$S_{E,C,b} = \frac{6\sigma_b}{d_{pb}^2} k_g Nu_b \left(T_b - T_g\right) \tag{20}$$

$$S_{E,C,h} = \frac{6\sigma_h}{d_{ph}^2} k_g Nu_h \left(T_h - T_g\right) \tag{21}$$

where the Nusselt number was calculated using the standard Ranz correlation:

$$Nu_i = 2 + 0.66\,\mathrm{Re}_i^{1/2}\,\mathrm{Pr}_g^{1/3} \tag{22}$$

The heat exchange between gas phase and biomass particles by product release was calculated by:

$$S_{E,P} = R_{b\to g}\left(c_{p,g}T_g - c_{p,b}T_b\right) \tag{23}$$

The thermal radiation of biomass and inert heating particles were calculated by:

$$S_{E,Rd,i} = -\frac{6\sigma_i}{d_{pi}}\left(\sigma_B T_i^4 - \pi\frac{I_x + I_y + I_z}{3}\right) \quad (24)$$

where σ_B is the Stefan Boltzmann constant.

The heat of reaction of biomass was calculated by:

$$S_{E,\mathrm{Re}} = \sigma_b \rho_b \sum_j R\Delta H_{\mathrm{Re}} \quad (25)$$

2.3 Gasification kinetics and conservation of each species

The dried biomass was assumed to consist of cellulose, hemicellulose and lignin. The products included char, tar and syngas. The syngas was assumed to consist of CO, CO_2, CH_4, and H_2. Each of the biomass components independently undergoes the same reaction pathway (Miller and Bellan, 1997; Jennen et al., 1999). The biomass was modeled as a solid reaction matrix where the void volume formed by pores was filled with gas. In the gasifier, three different kinds of reactions appeared simultaneously: pyrolysis, gas-phase, and gas-solid reactions.

In the pyrolysis of biomass particles, the volatiles were set free (Miller and Bellan, 1997; Varhegyi et al., 1997) according to:

$$\text{primary component} \xrightarrow{K_{p1}} \text{active(s)} + \Delta H_{p1}$$

$$\text{active} \xrightarrow{K_{p2}} \text{tar(g)} + \Delta H_{p2}$$

$$\text{active} \xrightarrow{K_{p3}} X\,\text{char(s)} + (1-X)\,\text{gas(g)} + \Delta H_{p3}$$

$$\text{tar(g)} \xrightarrow{K_{p4}} \text{gas(g)} + \Delta H_{p4}$$

where $X_c = 0.35$, $X_h = 0.60$ and $X_l = 0.75$.

The gaseous components continued reacting in the gas phase (Jennen et al., 1999) according to:

$$CO + 0.5O_2 \xrightarrow{K_{g1}} CO_2 + \Delta H_{g1}$$

$$H_2 + 0.5O_2 \xrightarrow{K_{g2}} H_2O + \Delta H_{g2}$$

$$CO + H_2O \xleftrightarrow{K_{g3}} CO_2 + H_2 + \Delta H_{g3}$$

$$\text{Tar} \xrightarrow{K_{g4}} \varphi_1 C + \varphi_2 H_2 + (1-\varphi_1-\varphi_2)CO + \Delta H_{g4}$$

The char (carbon) produced by the pyrolysis reaction reacted with the gaseous components (Wang Kinoshita, 1993) following:

$$C + H_2O \xrightarrow{K_{s1}} CO + H_2 + \Delta H_{s1}$$

$$C + CO_2 \xrightarrow{K_{s2}} 2CO + \Delta H_{s2}$$

$$C + \frac{1}{\varphi} O_2 \xrightarrow{K_{s3}} (2 - \frac{2}{\varphi})CO + \left(\frac{2}{\varphi} - 1\right)CO_2 + \Delta H_{s3}$$

$$C + 2H_2 \xrightarrow{K_{s4}} CH_4 + \Delta H_{s4}$$

In the above reaction formulae, k is the reaction constant and ΔH is the reaction heat. All reactions were assumed to be the first order and the reaction rate was given by:

$$R_j = K_j X_j \tag{26}$$

where K_j is the reaction constant and X_j is the mass fraction of the jth species.

The temperature-dependent reaction constant was calculated using Arrhenius equation:

$$K_j = K_{j0} e^{-\frac{E}{RT}} \tag{27}$$

The values of rate constant, K_{j0}, activation energy, E, and reaction heat, ΔH of each reaction were taken from literatures (Blasi, 1996; Varhegyi et al., 1997; Lathouwers and Bellan, 2001; Lv et al., 2003).

The gas phase included species such as H_2, CO, CH_4, CO_2, N_2, O_2 and H_2O. During gasification, the mass of each species was conserved, which was expressed as:

$$\frac{\partial}{\partial t}\left(\sigma \rho m_j\right)_g + \nabla \cdot \left(\sigma \rho U m_j\right)_g = \nabla \cdot \left(\sigma \rho D \nabla m_j\right)_g + R_{b \to g,j} + R_{g \to g,j} \tag{28}$$

where $R_{b \to g,j}$ and $R_{g \to g,j}$ are the average production rate of the jth species due to the solid phase reaction and the gas phase reaction.

2.4 Initial and boundary conditions

The initial velocities of all phases were set to be zero. The initial void fractions of the section loaded with bed material and the rest section in the gasifier were 0.4 and 1.0, respectively. The void fractions were initially filed with fluidizing gas. The inert heating material and the entrapped gas were initially preheated to the temperature of wall. The initial temperature of biomass was its inlet temperature.

The gas flow was assumed to be uniform over the bottom of the domain. The turbulent intensity of the inlet gas streams was assumed to be 10% of the inlet velocities and the value

of *k* at the inlet of gas was thus 1% mean kinetic energy of coming flow. The value of ε was calculated by $\mu_T = \rho_g C_\mu k^2 / \varepsilon$ and the value of μ_T was roughly estimated by $\rho_g u D_b / \mu_T = 100 \sim 1000$. The boundary conditions are given in Table 2.

Table 2. Boundary conditions for the model

	Bottom (Inlet of gas)	**Top (free surface)**	**Circumference of gasifier**	**Inlet of biomass**
Gas	$w_g = w_{g,I}$ $u_g = v_g = 0$ $m_{g,j} = m_{g,j,I}$ $T_g = T_{g,I}$	$P = P_{atm}$ $\frac{\partial w_g}{\partial n} = \frac{\partial u_g}{\partial n} = \frac{\partial v_g}{\partial n} = 0$ $\frac{\partial m_{g,j}}{\partial n} = 0$ $\frac{\partial T_g}{\partial n} = 0$	$w_g = 0$ $\frac{\partial u_g}{\partial n} = \frac{\partial v_g}{\partial n} = 0$ $\frac{\partial m_{g,j}}{\partial n} = 0$ $T_g = T_w$	$w_g = 0$ $\frac{\partial u_g}{\partial n} = \frac{\partial v_g}{\partial n} = 0$ $\frac{\partial m_{g,j}}{\partial n} = 0$ $T_g = T_{b,I}$
Biomass	$\frac{\partial w_b}{\partial n} = 0$ $u_b = v_b = 0$ $m_{b,j} = 0$ $\frac{\partial T_b}{\partial n} = h(T_b - T_{g,I})$	$\frac{\partial w_b}{\partial n} = \frac{\partial u_b}{\partial n} = \frac{\partial v_b}{\partial n} = 0$ $\frac{\partial m_{b,j}}{\partial n} = 0$ $\frac{\partial T_b}{\partial n} = 0$	$w_b = 0$ $u_b = v_b = u_{b.I}$ $m_{b,j} = m_{b,j,I}$ $\frac{\partial T_b}{\partial n} = 0$	$w_b = 0$ $\frac{\partial u_b}{\partial n} = \frac{\partial v_b}{\partial n} = 0$ $\frac{\partial m_{b,j}}{\partial n} = 0$ $T_b = T_{b,I}$
Inert heating materials	$\frac{\partial w_h}{\partial n} = 0$ $u_h = v_h = 0$ $\frac{\partial T_h}{\partial n} = h(T_h - T_{g,I})$	$\frac{\partial w_h}{\partial n} = \frac{\partial u_h}{\partial n} = \frac{\partial v_h}{\partial n} = 0$ $\frac{\partial T_h}{\partial n} = 0$	$w_h = 0$ $\frac{\partial u_h}{\partial n} = \frac{\partial v_h}{\partial n} = 0$ $T_h = T_w$	$w_h = 0$ $\frac{\partial u_h}{\partial n} = \frac{\partial v_h}{\partial n} = 0$ $T_h = T_w$

2.5 Finite element analysis of the model

Solutions to the model obtained the values of independent variables such as pressure, velocity, temperature and composition. The governing equations of momentum, energy and mass conservations were generally expressed as:

$$\frac{\partial}{\partial t}(\sigma\rho\phi) + \nabla \cdot (\sigma\rho U\phi) = \nabla \cdot (\Gamma \nabla \phi)_g + S_\phi \tag{27}$$

Closed-form solutions of the governing equations were difficult to develop. The governing equations were thus transferred to their corresponding finite element formulations and the values of the independent variables were found at a finite number of locations in the domain as shown in Figure 2.

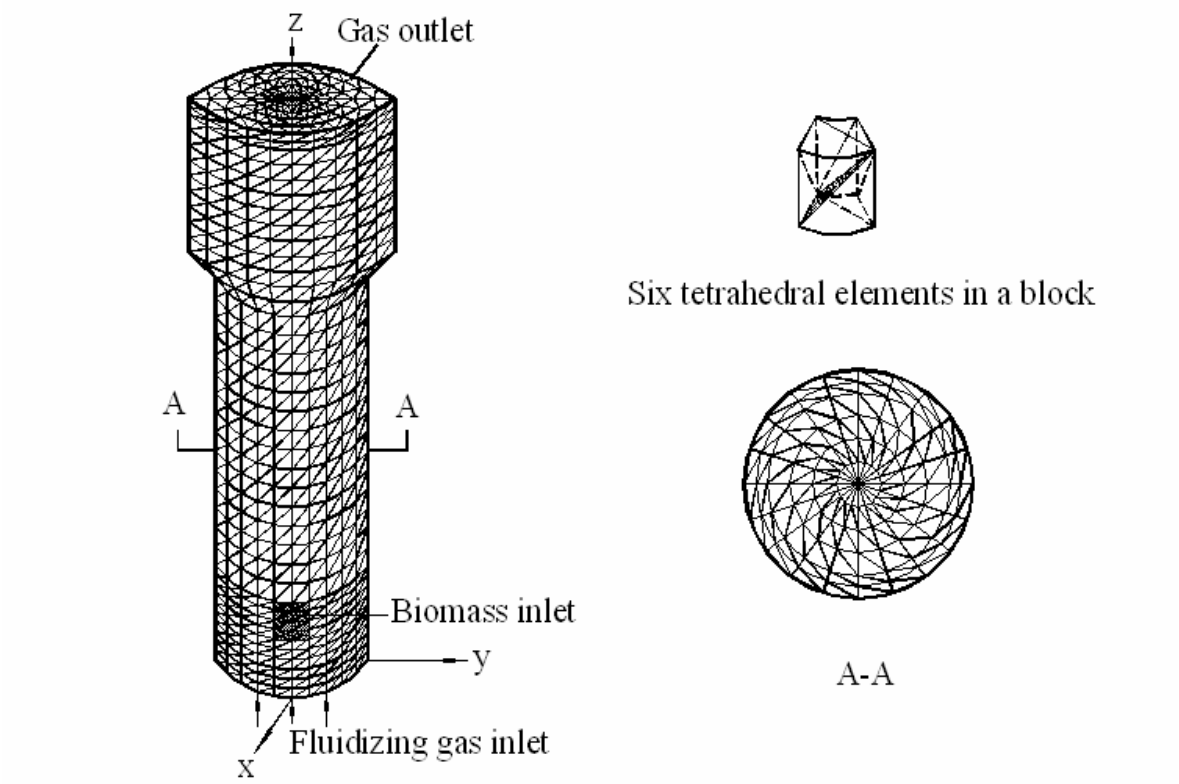

Figure 2. Finite element arrangement for the fluidized bed.

The finite element formulation was expressed as:

$$[M]\left\{\frac{\partial \phi}{\partial t}\right\}+[K]\{\phi\}=\{f\} \tag{28}$$

where [K] is the global conduction matrix, [M] is the global capacitance matrix and {f} is the global load vector. The set of transient differential equations (28) was solved by a finite difference scheme given by

$$\left(\frac{[M]}{\Delta t}+\alpha[K]\right)\{\phi\}_{n+1}=\left(\frac{[M]}{\Delta t}-(1-\alpha)[K]\right)\{\phi\}_n+\{f\}_n \tag{29}$$

where α is a weighting factor, which must be chosen in the interval between 0 and 1.

2.6 Computer program and model input

An object-oriented computer program was developed in Visual C++ to solve the model. The program has a user-friendly interface as shown in Figure 3. The interface includes six parts for users to input the parameters of gasifer geometry, biomass, fluidizing gas, inert heating material, finite element arrangement and simulation control.

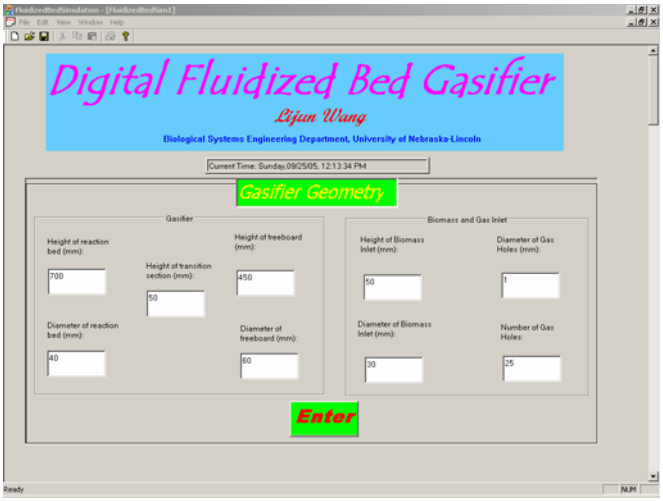

(a) Gasifier geometry

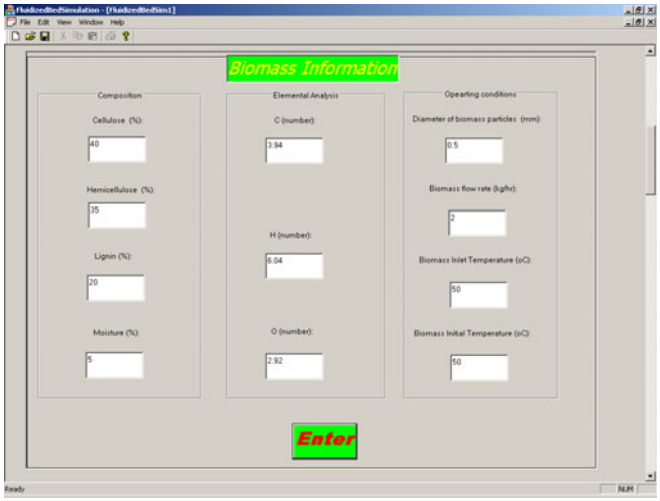

(b) Biomass

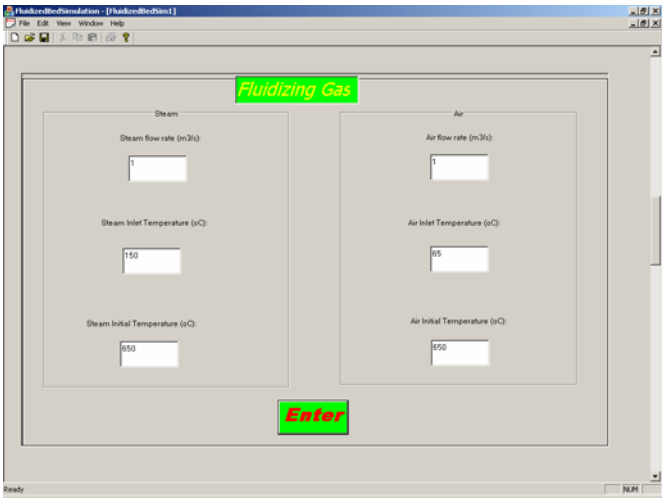

(c) Fluidizing gas

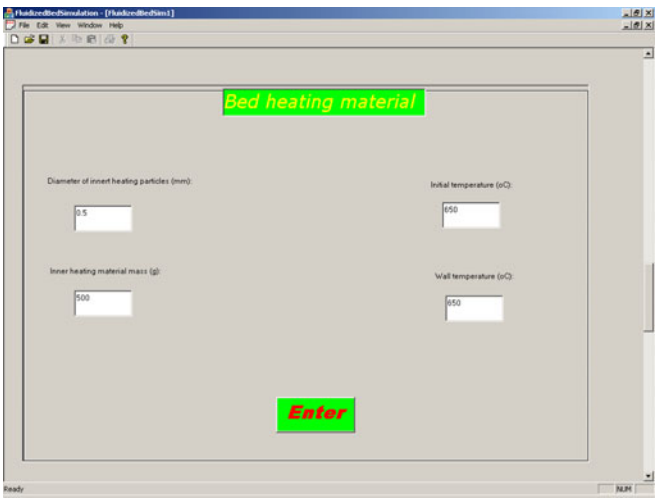

(d) Bed heating material

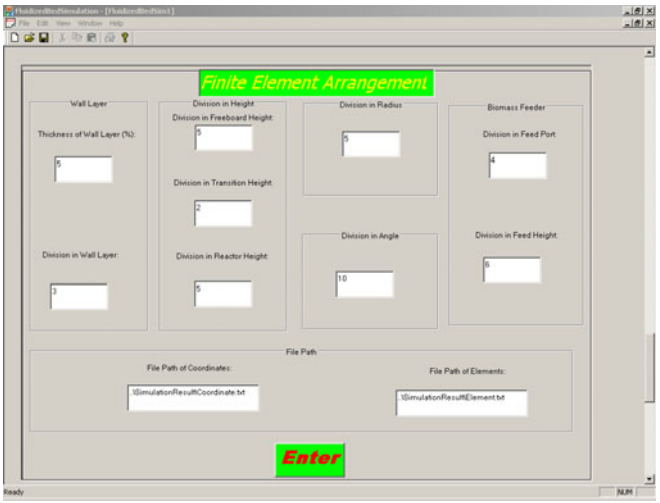

(e) Finite element arrangement

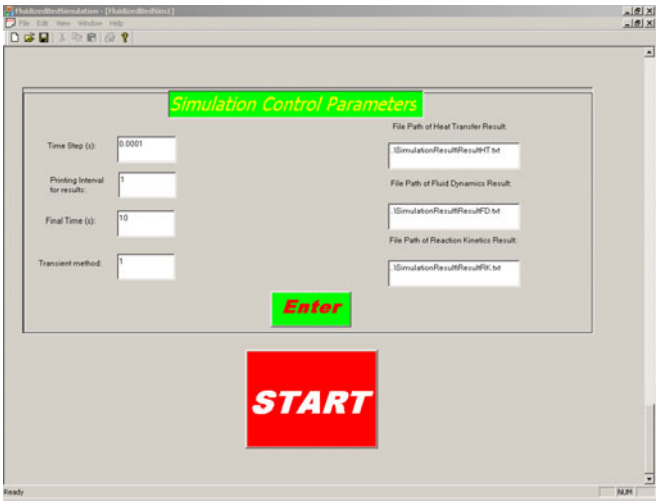

(f) Simulation control

Figure 3. Interface of the simulation program

The difficulty in finding the solution of the continuity and momentum equations was that the pressure in the momentum equation was implicit. An iterative solution strategy was used to find the velocity and pressure fields (Versteeg and Malalasekera, 1995).

3. Materials and Methods

3.1 Sorghum DDG Particles

The biomass used in this research was grain sorghum DDG. Sorghum DDG used in this research was obtained from an ethanol production facility, U.S. Energy Partners (Russsell, Kansas), using mixed commercial grain sorghum hybrids. Particle size distribution in the DDG was measured using a sieve shaker (Ro-TAP, W.S. Tyler, Cleveland, Ohio) equipped with six sieves (U.S. standard sieve Nos. 12, 14, 16, 20, 35 and 140) and a pan. The moisture content of DDG was measured using a moisture analyzer at the chamber temperature of 105^{o}C (HG 53 moisture analyzer, Mettler-Toledo GmbH, Laboratory & Weighing Technologies, Greifensee, Switzerland). The measurements of particle size distribution and moisture content of DDG were carried out in triplicate.

3.2 Fluidized Bed Gasification System

A laboratory fluidized bed gasification system was constructed as shown in Figure 4. The system contained a 316 stainless tube as the gasifer. The total length of the gasifier was 1,200 mm. The gasifier had a bed reactor section of 40 mm inner diameter at the bottom and freeboard section of 60 mm inner diameter at the top. The gasifier was heated using an electric tube furnace with a temperature controller. At the bottom of the gasifier, the fluidizing air and steam were uniformly distributed into the gasifier through a distribution plate of 13 mm thickness and with 25 holes of 1 mm diameter. The air was supplied by an air compressor and preheated to 65^{o}C before entering the gasifier. The steam of 150^{o}C came from a steam generator. Biomass was fed to the gasifier using a screw feeder driven by a variable speed motor to obtain different feeding rates. The feeding port of biomass was located 50 mm above the distribution plate. After the product gas exited the gasifier, it passed through a cyclone to remove fine particles in the gas flow. The temperature of cyclone was maintained above 200^{o}C to prevent any condensation of liquids from the gas. The gas further passed through a condenser to remove steam and tar, and through a cotton filter to remove any water in the gas.

The fluidized bed was charged with 100 g sand of 0.5 mm equivalent diameter as the bed material to enhance the stability of fluidization and heat transfer. The bed temperature ranged from 600^{o}C to 850^{o}C. The mass flow rate of biomass was varied between 0.5 and 2.5 kg/hr. The ratio of steam to biomass was varied between 0.5 and 2.0. The equivalent ratio (ER), which is the actual oxygen-to-fuel ratio divided by the stoichiometric oxygen-to-fuel ratio needed for complete combustion, was set at 0.10, 0.25, and 0.5. The superficial velocity of fluidizing gas was set between 0.5 m/s and 0.8 m/s. Before experiments, the gasifier bed was preheated to the set value. The air and steam at their set temperatures were distributed into the gasifier. After the bed temperature returned to its set value, the biomass was fed into the gasifer and a gasification test was started. The tests were conducted in triplicate at a 5 min interval.

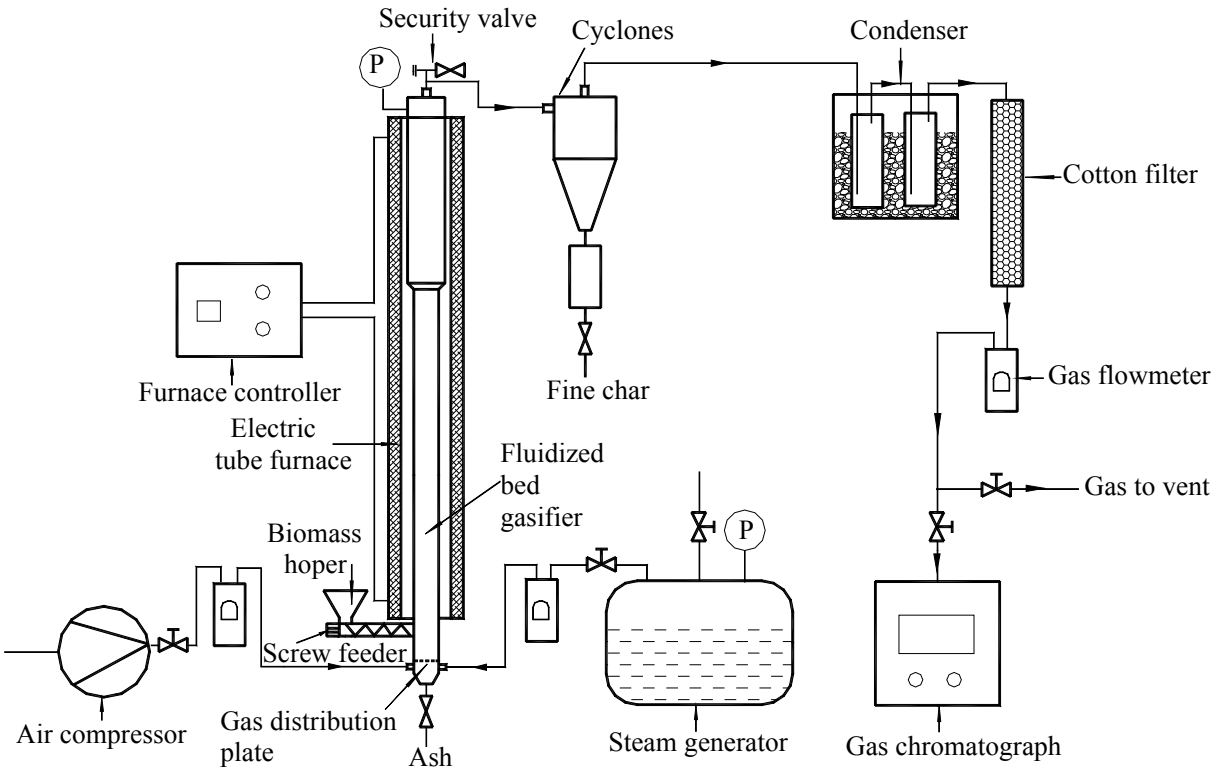

Figure 4. Schematic diagram of the fluidized bed gasification system.

The temperatures of gas at the inlet and outlet of the gasifier and cyclone were recorded using K-type thermocouples. Temperatures were also measured at points along the gasifier height at 100 mm intervals using K-type thermocouples to obtain the temperature distribution in the gasifier. The flow rates of air and steam were measured using two flow rate meters. The quantity of char was obtained by weighing the bed materials before and after gasification. The quantity of dry gas produced was measured at the exit containing a cotton filter by means of a volumetric gas-meter. The gas composition was determined using a gas chromatograph with a TCD detector. Standard gas mixtures were used for quantitative calibration.

4. Results and Discussion

Simulation has initially been performed on a Pentium 4 CPU (2.66 GHz) with 1.5GB RAM. Due to the restriction of available computational power, only the reaction section of 40 mm I.D. $\times$ 700 mm length and initial pyrolysis were considered in this simulation. The computational domain was divided into 16,470 elements connected with each other by 3,162 nodes. The mesh density at the inlets of biomass and gas, and a layer near the wall was increased. The time step was set at 10^{-3} s for the computation of heat transfer and reaction, and 1 s for the computational fluid dynamics. It took 20 hours per run for a 10 second physical process. The predicted velocity and temperature profiles along the fluidized bed over computed time are shown in Figures 5 and 6. On each cross sectional plate along the bed, the average values were used in the figures. More simulation will be carried out in the near future.

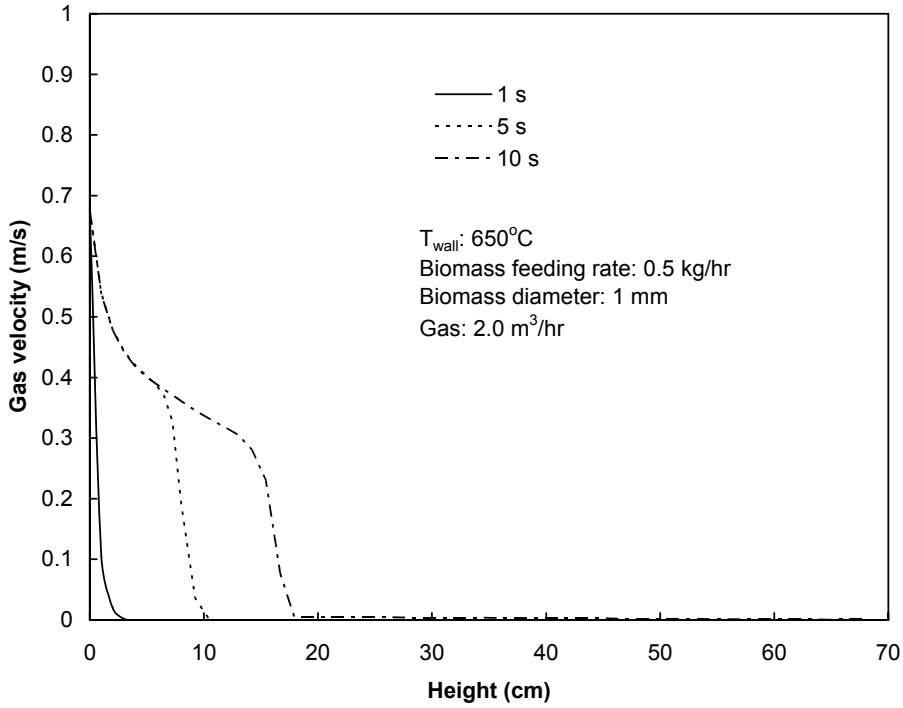

Figure 5 Gas velocity profile along the fluidized bed over computed time.

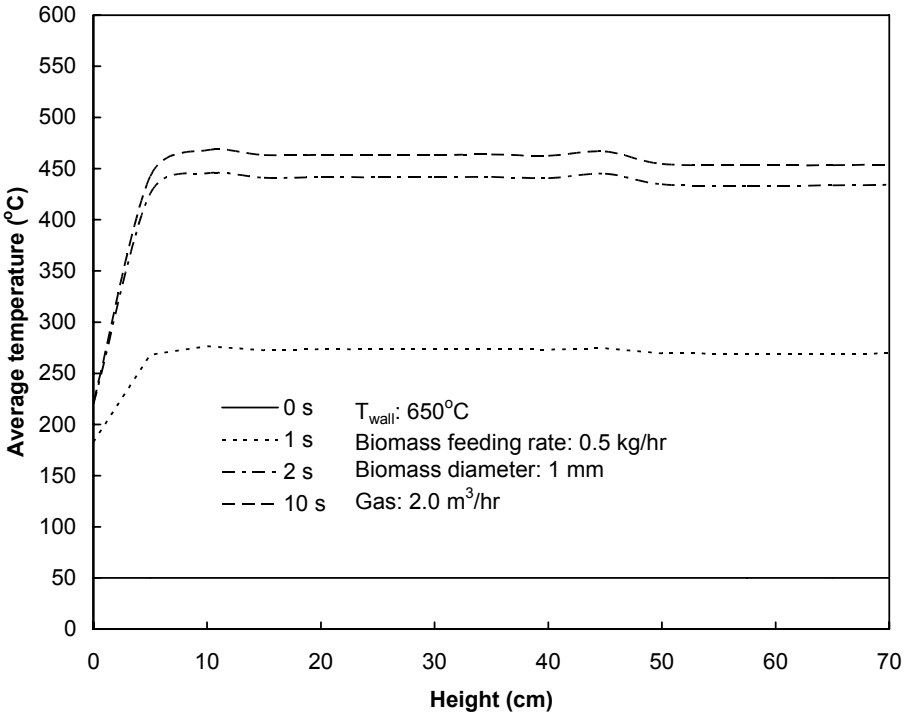

Figure 6 Biomass temperature profile along the fluidized bed over computed time.

5. Conclusions and future work

A transient and three-dimensional mathematical model of fluid dynamics, heat transfer and reaction kinetics has been developed. The model was solved using a finite element method. A user-friendly computer program was developed to implement the model. Experiments will be carried out to validate the model. The validated model will be used to investigate the relationship among raw biomass, gasifer and products for the improvement of production efficiency and product quality.

Nomenclature

C_d drag coefficient

c_p specific heat (J/kg K)

D diffusity

d_p diameter of biomass or inert heating particles (m)

E activation energy

G turbulence production term

ΔH reaction heat (J/mole)

K reaction rate constant

k thermal conductivity (W/mK)

m mass (kg)

M_g average molecular weight (kg/mol)

Nu Nusselt number

P pressure (Pa)

Pr Prandtl number

R gas constant (J/mol K)

R_{bj} reaction rates of the j^{th} component in biomass (kg reacted component /s·kg biomass)

Re Reynolds number

S_E body energy source (w/m^3)

S_F external body forces (N/m^3)

$S_{M,i}$ the ith phase external mass sources (kg/m^3s)

T temperature (K)

t time (s)

u velocity in the x direction (m/s)

U velocity vector (m/s)

v velocity in the y direction (m/s)

w velocity in the z direction (m/s)

Subscripts

b biomass

C convection

F force

g gas

h inert heating particles

i the ith phase

j the jth species

M mass

p pyrolysis

P product

Rd radiation

Re reaction

s solid

T turbulence

Greek letters

σ volumetric fraction of each phase

ρ density (kg/m^3)

ε turbulent dissipation

κ turbulent kinetic energy

σ_B the Stefan Boltzmann constant

μ_e efficient turbulent viscosity (Pa s)

References

Blasi C. D. (1996). Kinetic and heat transfer control in the slow and flash pyrolysis of solids. Ind. Eng. Chem. Res. 35: 37-46.

Huang, J.; Fang, Y.; Chen, H. and Wang, Y. (2003). Coal gasification characteristic in a pressurized fluidized bed. *Energy & Fuels*, 17: 1474 – 1479.

Ishii, M. and Zuber, N. (1979). Drag coefficient and relative velocity in bubbly, droplet or particulate flows. AIChE Journal, 25 (5): 843-855.

Jennen, T.; Hiller, R.; Koneke, D. and Weinspach, P.M. (1999). Modleing of gasification of wood in a circulating fluidized bed. Chemical Engineering Technology, 22: 822-826.

Lanzetta M and Blasi, C. D. (1998). Pyrolysis kinetics of wheat and corn straw. Journal of Analytical Applied Pyrolysis, 44: 181-192.

Lathouwers D. and Bellan J. (2001). Modeling of biomass pyrolysis for hydrogen production: the fluidized bed reactor. *The Proceeding of the 2001 DOE Hydrogen Program Review*, the U. S. Department of Energy.

Lv, P.; Chang, J.; Xiong, Z.; Huang, H.; Wu, C.; Chen, Y. and Zhu, J. (2003). Biomass air-steam gasification in a fluidized bed to produce hydrogen-rich gas. *Energy & Fuels*, 17: 677 – 682.

Rapagna S.; Jand N.; Kiennemann A. and Foscolo P.U. (2000). Steam-gasification of biomass in a fluidized-bed of olivine particles. *Biomass and Bioenergy,* 19: 187 – 197.

Scott D.S.; Majerski P.; Piskorz J.; Radlein D. (1999). A second look at fast pyrolysis of biomass-the RTI process. Journal of Analytical and Applied Pyrolysis, 51: 23-37.

Varhegyi G.; Antal M.J.; Jakab E.; Szabo P. (1997). Kinetic modeling of biomass pyrolysis. Journal of Analytical and Applied Pyrolysis, 42: 73-87.

Versteeg, H.K. and Malalasekera, W. (1995). An Introduction to Computational Fluid Dynamics- The Finite Volume Method, Longman Group Ltd., London. p.10 – 24, 135 - 150.

Wang, L. L., Weller, C. L. and Hwang, K.T. 2005. Extraction of lipids from grain sorghum DDG. Transactions of the ASAE. In press.

Wang, Y., Kinoshita, C. M. Kinetic model of biomass gasification, Solar Energy, 51, 1993, 19-24.

Wu, J.; Fang, Y.; Wang, Y. and Zhang D.K. (2005). Combined coal gasification and methane reforming for production of syngas in a fluidized-bed reactor. *Energy & Fuels*, 19: 512 – 516.